FEBS Letters 584 (2010) 2271–2278

FEBS Letters

journal homepage: www.FEBSLetters.org

Targeted knock-out of a gene encoding sulfite reductase in the moss *Physcomitrella patens* affects gametophytic and sporophytic development

Gertrud Wiedemann [a], Corinna Hermsen [b,c], Michael Melzer [d], Annette Büttner-Mainik [a], Heinz Rennenberg [e], Ralf Reski [a], Stanislav Kopriva [c,*]

[a] University of Freiburg, Faculty of Biology, Plant Biotechnology, Schaenzlestrasse 1, 79104 Freiburg, Germany
[b] Martin Luther University Halle-Wittenberg, Department of Biochemistry/Biotechnology, Kurt-Mothes-Str. 3, 06120 Halle (Saale), Germany
[c] John Innes Centre, Norwich, NR4 7UH, UK
[d] Leibniz Institute of Plant Genetics and Crop Plant Research, D-06466 Gatersleben, Germany
[e] University of Freiburg, Faculty of Forestry and Environmental Sciences, Institute of Forest Botany and Tree Physiology, Tree Physiology, Georges-Köhler-Allee 53, 79085 Freiburg, Germany

ARTICLE INFO

Article history:
Received 26 September 2009
Revised 17 March 2010
Accepted 22 March 2010
Available online 30 March 2010

Edited by Michael R. Sussman

Keywords:
Bryophyte
Moss development
Protonema development
Spore maturation
Sulfate assimilation

ABSTRACT

A key step in sulfate assimilation into cysteine is the reduction of sulfite to sulfide by sulfite reductase (SiR). This enzyme is encoded by three genes in the moss *Physcomitrella patens*. To obtain a first insight into the roles of the individual isoforms, we deleted the gene encoding the *SiR1* isoform in *P. patens* by homologous recombination and subsequently analysed the Δ*SiR1* mutants. While Δ*SiR1* mutants showed no obvious alteration in sulfur metabolism, their regeneration from protoplasts and their ability to produce mature spores was significantly affected, highlighting an unexpected link between moss sulfate assimilation and development, that is yet to be characterized.

1. Introduction

Mosses have become an important group of plants for developmental studies, especially targeting evolutionary questions [1,2]. Among them *Physcomitrella patens* emerged as a powerful model species for molecular genetics, due to the high frequency of homologous recombination enabling gene targeting [3–5]. A large collection of genetics tools is available for *P. patens* including genome sequence, EST libraries, and a genetic map [6–9]. The simplicity of tissues and ease of cultivation under standardized conditions together with the reverse genetics tools also make *P. patens* attractive for studies of metabolism [1,10,11]. In *P. patens*, as in other mosses, the haploid gametophyte dominates the diploid sporophyte. The moss colonies are originally formed from chloronemal filaments with well-developed chloroplasts. Later, caulonema filaments are formed which enable spread of the colony. Some caulonema cells differentiate to buds which further develop to gametophores. At the tips of adult gametophores the sexual organs, antheridia (male) and archegonia (female), are produced under inducing conditions [12]. After fertilisation of the egg inside the archegonium a sporophyte develops which contains approx. 5000 spores [13]. The moss life cycle can be affected by phytohormones but also by metabolic processes [14–16].

P. patens has been widely used to address various questions of primary metabolism, such as fatty acid synthesis, *N*-glycosylation, or sulfur metabolism [10,11,17–20]. Many such analyses revealed an unexpected variety of enzymes and pathways alternative to those in flowering plants. These observations were corroborated by transcriptome analysis which showed that, whereas in seed plants 10–44% of genes are involved in metabolism, the proportion of metabolic genes in *P. patens* reaches 70–80% [21]. Analysis of sulfur metabolism in *P. patens* revealed that some metabolic steps are less complex in this moss than in seed plants, while others are more diverse in mosses [19]. For example, for the reduction of activated sulfate (adenosine 5′-phosphosulfate, APS) to sulfite, a novel form of APS reductase without an iron-sulfur cofactor was identified in *P. patens* [20,22]. Also, the reduction of sulfite to sulfide by sulfite reductase (SiR) is more complex in *Physcomitrella* than in seed plants. While this enzyme is encoded by a single copy gene in *Arabidopsis* and by a maximum of two copies in other seed plants, three isoforms of *SiR* are present in the *P. patens* genome [19].

* Corresponding author. Fax: +44 1603 450045.
E-mail address: stanislav.kopriva@bbsrc.ac.uk (S. Kopriva).

0014-5793/$36.00
doi:10.1016/j.febslet.2010.03.034

As a first step to address the biological function of the individual *SiR* genes we disrupted *PpSiR1* by homologous recombination. We found that despite minimal effects on sulfur metabolism the Δ*SiR1* plants show surprisingly strong developmental alterations and are unable to produce mature spores.

2. Materials and methods

2.1. Plant material

P. patens (Hedw.) B.S. was cultured in liquid or solid Knop medium as described earlier [23]. To study the effect of cadmium, protonema cultures in flasks were adjusted to a moss dry weight of 400 mg/L and the Knop medium was supplemented with 5 and 10 μM $CdCl_2$, respectively, for 10 days. Cadmium treatments were performed in two independent repetitions with three independent cultures each. The described ΔSiR1 mutants are deposited in the International Moss Stock Center with the accessions IMSC 40447 (1–6), IMSC 40450 (3–17), IMSC 40454 (4–5) and IMSC 40455 (5–15).

2.2. Production and selection of PpSiR1 knock-out moss

To create the *PpSiR1* knock-out construct the genomic DNA fragment containing part of the gene (1552 bp) was obtained by PCR with primers PPSIR1F and PPSIR1R (for primer sequences see Supplementary Table 1) cloned into the pCRII vector (Invitrogen, Karlsruhe, Germany) and sequenced. A 442 bp BstBI and BsrGI fragment was replaced with the nptII selection marker [10]. Thirty micrograms of the plasmid were cut with EcoRI, producing a 3 kb linear fragment which contained the nptII gene flanked by PpSiR1 genomic sequences of 590 bp and 517 bp. *P. patens* protoplasts were isolated and PEG-mediated transformation, regeneration, and selection were performed as described previously [24].

The screening of G418-resistant plants was performed as described in [17] with small pieces of gametophores and primers SIR1KO1 and SIR1KO2 to detect a disruption of the original *PpSiR1* gene, N1 and N2 to detect the presence of the *npt*II cassette, SIR1EN and N3, and N4 and SIR1EC to control the integration of the transgene at the 5′-end and the 3′-end, respectively (Fig. 2). Plants that gave the expected fragments in all four PCR reactions (1–6, 4–5, and 5–15) were selected for further analysis and liquid protonema cultures were established from these lines.

For analysis of the developmental phenotype protonema of WT moss and three Δ*SiR1* lines, 1–6, 4–5, and 5–15, protoplasts were isolated and grown in liquid regeneration medium for 10 days. After washing, the regenerating protoplasts were transferred to Knop medium. Samples for microscopic analysis were taken after 7, 14, 20, and 35 days. The number of cells per regenerating protoplast was counted 7 days after protoplast isolation for 1000 cells of each of the four genotypes. Presence of caulonema cells was examined 14 days after protoplast isolation for 300 regenerating filaments of each line.

2.3. Expression analysis

Total RNA from frozen moss protonema tissue of WT and Δ*SiR1* lines was isolated using the TRIZOL® Reagent (Invitrogen, Karlsruhe, Germany) according to the manufacturer's instructions. First strand synthesis was performed with Superscript II reverse transcriptase (Invitrogen, Karlsruhe, Germany) from 2 μg of total RNA. To verify lack of *SiR1* transcript in the knock-out lines reverse transcription PCR with primers SIR1KO1 and SIR1KO2 was performed according to a standard protocol. To verify that *PpSiR2* and *PpSiR3* are not affected in the Δ*SiR1* lines primer pairs SIR2F/SIR2R and SIR3F/SIR3R, respectively, were utilized. Primers for the constitutively expressed mRNA of the ribosomal protein L21 C45fw and C45rev were used as controls.

Semiquantitative RT-PCR was performed as described in [25] with primers specific for components of sulfate assimilation: five sulfate transporters, two isoforms of ATP sulfurylase, two isoforms of adenosine 5′-phosphosulfate reductase, and PpSiR2 and PpSiR3 (Supplementary Table 1). Preliminary experiments established reaction conditions to ensure that the reactions were still in exponential phase. Amplification with primers for the constitutively expressed TATA-binding protein TBPfw and TBPrev was used for normalization.

2.4. Southern blot analysis

Genomic DNA was isolated with a CTAB method. One microgram genomic DNA was digested for 16 h with 20 U of restriction enzymes EcoRI and Mph1103I (Fermentas, St. Leon-Rot, Germany). After electrophoresis, the DNA was transferred to positively charged nylon membrane (GE Healthcare, Munich, Germany). Hybridization and detection were performed as described in the Roche DIG Application Manual using hybridization and blocking solutions and Anti-digoxigenin-AP conjugate from Roche (Mannheim, Germany) and CDP-Star (GE Healthcare, Munich, Germany). Fluorescent bands were visualized on Lumi-Film Chemiluminescent Detection Film (Roche, Mannheim, Germany). DIG-labeled hybridization probe for detection of the *npt*II selection cassette were prepared by PCR-labeling from plasmid DNA of pRKO25.2 [4] with the primers PT1 (GAGGCTATTCGGCTATGACTG) and PT2 (ATCGGGAGCGGCGATACCGTA) using the random-primed labeling mix from Roche.

2.5. Western blot analysis

SiR protein accumulation was assessed by Western blotting with polyclonal antisera against recombinant SiR from *Arabidopsis* [26] using liquid culture grown protonema.

2.6. Chlorophyll measurements

Chlorophyll was extracted and quantified from 50 to 100 mg of blotted fresh moss protonema as described in [22].

2.7. HPLC analysis of low molecular weight thiols

The analysis of cysteine, γ-glutamylcysteine and GSH in 50–70 mg of blotted moss protonema from liquid culture was performed as described in [11].

2.8. Localization of SiR1, SiR2 and SiR3

The intracellular localization of SiR isoforms was addressed by transient expression of vectors encoding C-terminal green fluorescent protein (GFP) fusion proteins as described in [20]. The complete open reading frames of *PpSiR1*, *PpSiR2* and *PpSiR3* were fused to GFP reporter using the plasmid mAV4 [27]. As a control for plastid targeting, the plasmid pCTP-GFP [28] was used. The transfection and microscopy was performed as in [20].

2.9. DAPI staining of chloroplast nucleoids

The protonema of 2 ml liquid culture was sedimented by centrifugation for 5 min at 500 rpm. The plant material was fixed with 80 μl glutardialdehyde (Roth, Karlsruhe, Germany) in 1 ml Knop medium for 30 min. For the removal of this solution a centrifugation for 5 min at 500 rpm followed. Afterwards samples were

stained with 750 µl DAPI-solution (Roth, Karlsruhe, Germany) with a concentration of 2 µg/ml [29]. Before microscopic analysis the material was destained for 1 h 30 min in water.

2.10. Enzyme assays

APS reductase activity was determined as the production of [^{35}S]sulfite, formed in the presence of [^{35}S]APS and dithioerythritol [26]. To measure specifically APR-B 2 µg thioredoxin from *Escherichia coli* (Sigma–Aldrich, Gillingham, UK) were added to each assay, the concentration of APS was increased from 37.5 µM to 100 µM and $MgSO_4$ was exchanged for KNO_3 [22]. ATPS was measured as the APS and pyrophosphate-dependent formation of ATP [30]. The protein concentrations in protein extracts from liquid culture protonema were determined according to Bradford with bovine serum albumin as a standard.

2.11. Sulfate uptake

Sulfate uptake was measured using [^{35}S]sulfate with moss protonema grown on sterile cellophane disks (bioFOLIE; VivaScience, Göttingen, Germany) placed onto agarose plates containing Knop media.

2.12. Immunogold labeling

Gametophores of wild type *P. patens* and the Δ*SiR1* 4–5 line were processed for ultrastructural examination and immunogold labeling with antisera against recombinant ATPS1, APR, and SiR from *Arabidopsis* as described previously [31,32] A FEI Tecnai G20 transmission electron microscope at 120 kV was used for the analysis.

3. Results

3.1. The SiR multigene family of P. patens

Analysis of the genome sequence revealed that *P. patens* sulfite reductase (SiR) is encoded by three genes. The predicted isoforms are 83% identical on the amino acid level and possess approx. 68% and 70% identical amino acid residues with SiR from *Arabidopsis thaliana* and the lycophyte *Selaginella moellendorffii*, respectively. Sequence analysis suggests that all three SiR isoforms are localized in plastids, as is the case for the enzyme in seed plants. Plastidic localization was confirmed by confocal laser scanning microscopy (CLSM) of protoplasts expressing SiR::GFP fusion proteins (Fig. 1). The same co-localization was obtained with a control construct encoding GFP fused to the chloroplast targeting peptide of FtsZ2-1 [28]. The fluorescence signal of the PpSiR isoforms was not uniformly distributed within the plastids but was concentrated in multiple spots, similar to the localization APS reductase [20]. All three *SiR* genes are expressed in protonema and gametophores as revealed by EST databases and RT-PCR (data not shown).

3.2. Disruption of the PpSiR1 gene

As the first step to address the biological function of individual *SiR* genes we analysed the effects of loss of function of *PpSiR1*. The

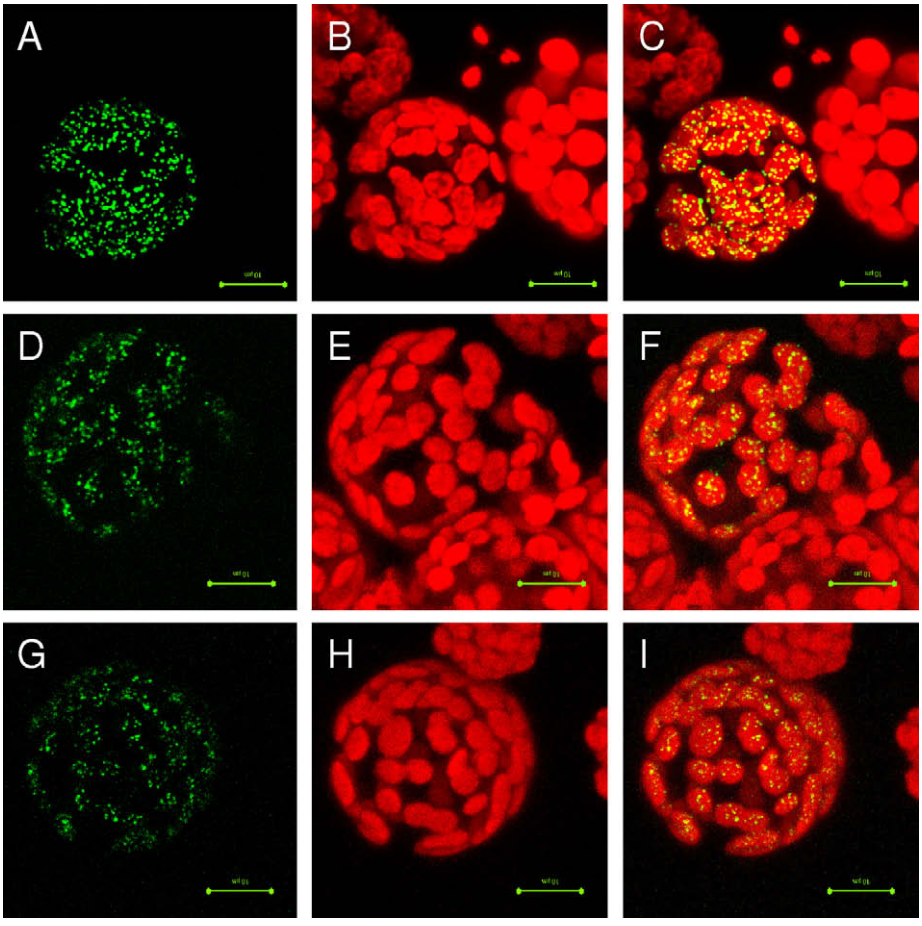

Fig. 1. Subcellular localization of *P. patens* SiR. *P. patens* protoplasts were transfected with expression constructs encoding C-terminal fusions of GFP to PpSiR1 (A–C), PpSiR2 (D–F), PpSiR3 (G–I). Presented are CLSM images 5 days after transfection. (A, D and G), GFP fluorescence, (B, E and H), chlorophyll autofluorescence, and (C, F and I), merge of both channels. The bar represents 10 µm.

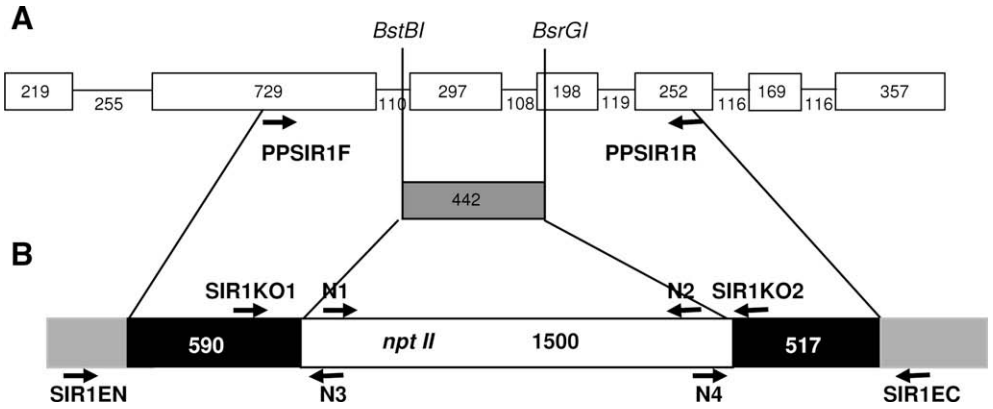

Fig. 2. (A) Schematic representation of the *PpSiR1* gene. The rectangles represent exons, introns are presented as lines. The numbers represent the length in base pairs. The positions of the *Bst*BI and *Bsr*GI sites, used to cut out the 442 bp fragment and replace it with the *npt*II cassette, are indicated. (B) The *PpSiR1* disruption construct. The positions of the PCR primers are indicated by arrows.

PpSiR1 gene is 3041 bp long and consists of seven exons and six introns (Fig. 2). After transformation with the knock-out construct, 78 regenerated G418-resistant moss colonies were screened by PCR with four different primer pairs to identify positive recombination events. For nine transformants all four PCR reactions resulted in the expected products indicating that they represent true knock-outs of the *PpSiR1* gene. Indeed, no *PpSiR1* transcript was detected in liquid protonema cultures of these transformants by RT-PCR with primers SIRKO1 and SIRKO2 (Fig. 3A). The transcripts of *PpSiR2* and *PpSiR3* were present in the Δ*SiR1* plants, showing that only a single *SiR* gene was disrupted (Fig. 3B). Western analysis with antibodies against SiR from *A. thaliana* showed the same amount of SiR protein in the knock-out mutants compared to wildtype, indicating a compensation of the disrupted gene at the transcriptional or translational level (Fig. 3C). However, this compensation has to be verified by an independent quantitative immunoassay, e.g., competitive ELISA. Southern analysis revealed that while the lines 3–17, 4–5, and 5–15 possess multiple copies of the transgene, the number is very low in the line 1–6 (data not shown). The high number of transgenes is usually caused by concatenation of the DNA and insertion of multiple copies at the targeted site or less frequently by a non-homologous recombination [5]. Since the Δ*SiR1* lines resulted from independent transformation events, it is extremely unlikely that the same genes would be disrupted in a non-targeted manner and thus any metabolic and/or developmental alterations can be directly linked to the disruption of *SiR1*.

3.3. Effect of PpSiR1 disruption on sulfate metabolism

Neither concentration of glutathione and cysteine nor the glutathione redox state were affected in liquid protonema cultures of the three independent Δ*SiR1* lines compared to WT plants (Table 1). The enzyme activities of ATP sulfurylase and the two isoforms of APS reductase as well as sulfate uptake rate were also not affected in the Δ*SiR1* mutants (Fig. 4). Steady state mRNA levels of sulfate transporters *Sultr1;1* and *Sultr1;3* were significantly reduced by 25–30% in all three lines, while *Sultr4;1* was significantly increased in two of the three lines (Fig. 4). The mRNA for the *ATPS2* isoform of ATP sulfurylase and the *APR-B* isoform of APS reductase were slightly but significantly reduced in all three lines, while the higher plants-like *APR* transcript level was reduced in two lines. The transcript levels of *SiR2* were not affected and *SiR3* was significantly reduced in all three Δ*SiR1* lines (Fig. 4).

Sensitivity to the toxic heavy metal cadmium is a typical consequence of disturbance of sulfur metabolism in *P. patens* [11,22].

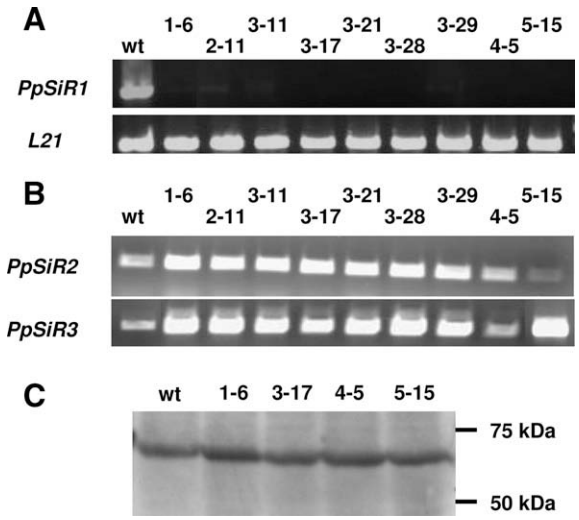

Fig. 3. (A) Expression analysis of *PpSiR1* and ribosomal protein L21, as a control, in wild type *P. patens* and 9 putative Δ*SiR1* lines. (B) RT-PCR of *PpSiR2* and *PpSiR3* in the same lines. (C) Western blot analysis of protein extracts from WT moss and 4 Δ*SiR1* lines with antibodies against recombinant SiR from *A. thaliana*.

Table 1
Levels of low molecular weight thiols and redox state in WT and Δ*SiR1* lines. Content of low molecular thiols and redox state in moss protonema grown in liquid Knop medium was determined by HPLC. The data in (nmol/g fresh weight) for thiols and ratio of GSSG/total glutathione for redox state are presented as average ±S.D. from three independent cultures for each line.

	wt	Δ*SiR*1–6	Δ*SiR*3–17	Δ*SiR*4–5	Δ*SiR*5–15
GSH	433 ± 170	466 ± 104	421 ± 97	529 ± 102	368 ± 58
Cysteine	68 ± 10	59 ± 9	54 ± 9	69 ± 14	52 ± 7
GSSG	66 ± 26	74 ± 34	84 ± 27	95 ± 51	79 ± 59
Redox state	0.17 ± 0.05	0.16 ± 0.05	0.21 ± 0.03	0.17 ± 0.06	0.2 ± 0.14

However, no differences in chlorophyll contents, as a measure of cell vitality, were found among protonema of WT moss and three independent Δ*SiR1* lines grown in liquid culture in the presence of 5 μM or 10 μM $CdCl_2$ (data not shown). This result indicates a compensation of the loss of function of the *PpSiR1* gene by the other isoforms, as already indicated by equal amounts of SiR protein in Western blots.

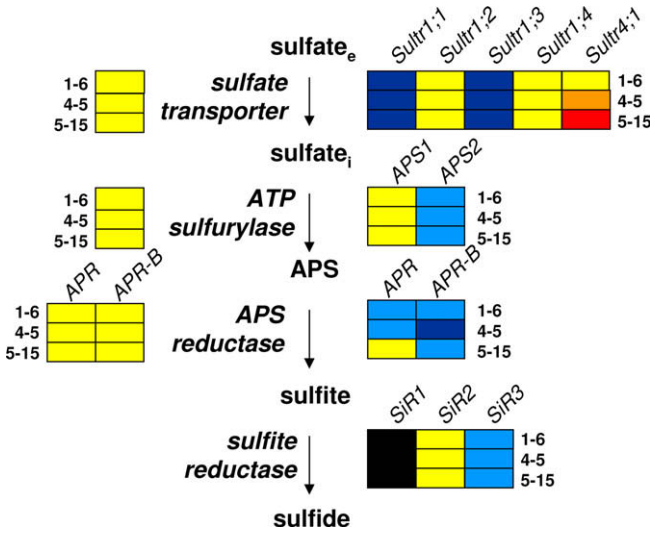

Fig. 4. Comparison of sulfate transport, ATP sulfurylase, APR, and APR-B activities (left) and transcript levels of genes involved in sulfate uptake and assimilation (right) in protonema of wild type moss and Δ*SiR1* lines 1–6, 4–5, and 5–15. Results are presented as a heat map: rectangles denote individual genes or enzymes encoding components of sulfate assimilation in the individual KO lines. Dark blue represents transcripts significantly reduced compared to WT by >25%, light blue transcripts reduced by <25%, red denotes increase by >25%, and orange increase by <25%. Yellow represents no difference in expression or activity, and black is the PpSiR1 transcript missing in the mutants.

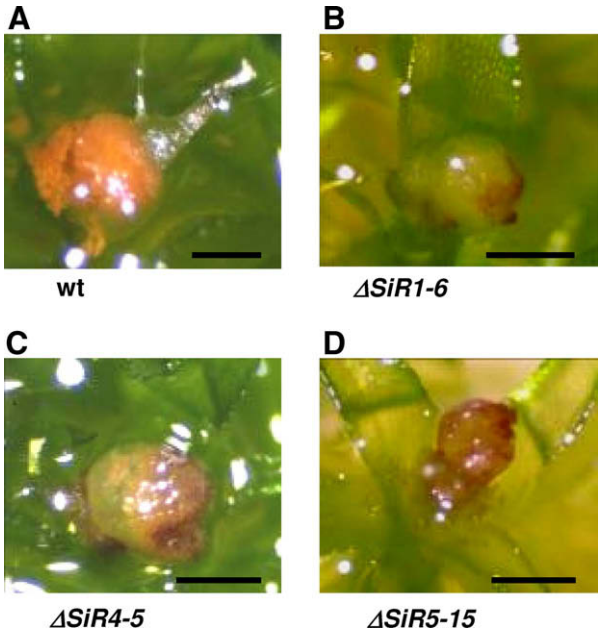

Fig. 6. Sporophytes of *P. patens* WT (A) and Δ*SiR1* (B–D) lines 8 weeks after induction of sporulation by flooding. The spores of WT plants develop until they are mature in the spore capsules which then tear open and set free the spores. In the Δ*SiR1* lines the spore capsules crack open when the spores inside are still immature. Size bars represent 100 μm.

3.4. Developmental phenotype of ΔSiR1 plants

In contrast to the Δ*APR* or Δ*APR-B* plants [11,22] which did not display any growth or developmental phenotype under standard conditions, the Δ*SiR1* mutants were significantly different from WT moss. The regeneration of protoplasts derived from Δ*SiR1* was slower than from WT. In regenerating protoplasts of WT the cell number appeared to be higher than in those from three independent Δ*SiR1* lines after 7 days (Fig. 5A). Indeed, more than 60% of WT cells were divided whereas only half of cells derived from the three Δ*SiR1* lines (Fig. 5B) undertook cell division. After 14 days on solid Knop plates the WT plants showed extensive secondary branching whereas only few and solely primary branches appeared on the Δ*SiR1* filaments. Consequently, WT tissue was formed

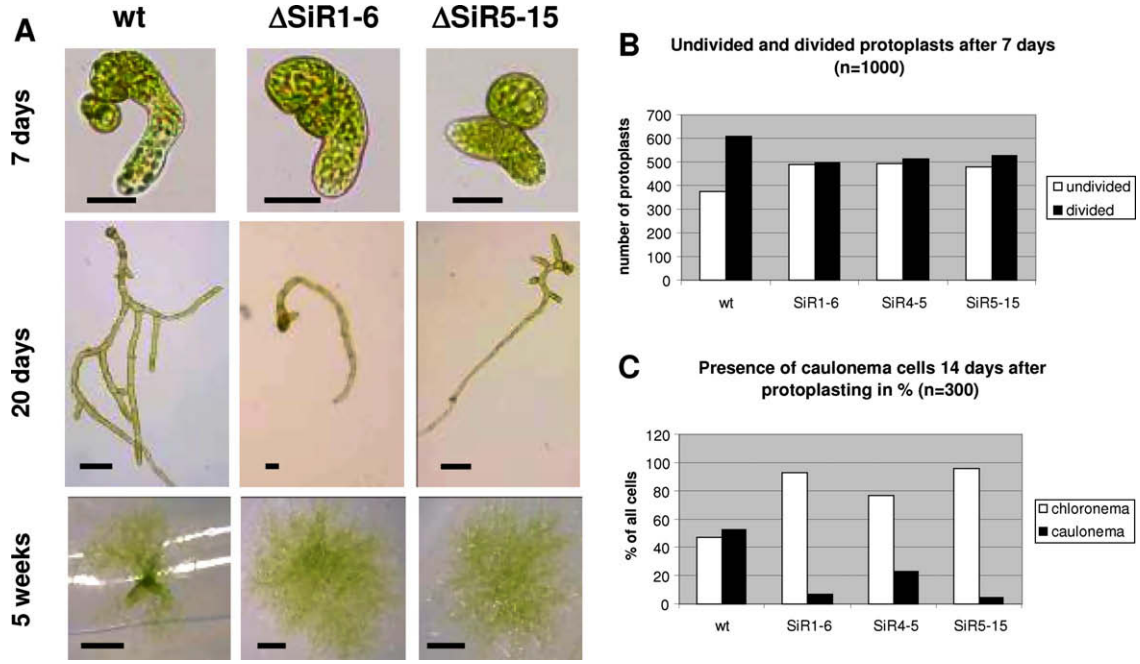

Fig. 5. (A) Light microscopy pictures of regenerating protoplasts of WT and the Δ*SiR1* lines 1–6 and 5–15 7 days and 20 days after protoplast isolation (scale bars represent 100 μm). After 10 days some of the plants were transferred to solid Knop medium covered with cellophane. Five weeks after protoplast isolation the WT plants developed leaves while the Δ*SiR1* plants still grew as protonema (scale bars represent 500 μm). (B) Numbers of divided and undivided cells per regenerating protoplast were counted 7 days after protoplast isolation for WT and 3 Δ*SiR1* lines ($n = 1000$). (C) Presence of caulonema cells in colonies of regenerating filaments was examined 14 days after protoplast isolation ($n = 300$).

Table 2
Number of sporophytes per 20 plants eight weeks after induction.

wt	Δ*SiR*1–6	Δ*SiR*4–5	Δ*SiR*5–15
33	9	8	7

approximately from the same number of chloronema and caulonema cells, while only few cells in the Δ*SiR1* plants underwent differentiation to caulonema (Fig. 5C). Thirty five days after protoplast isolation, the WT moss colonies formed gametophores whereas those derived from the Δ*SiR1* lines were still growing as protonema (Fig. 5A).

When sexual reproduction was induced in the different lines [12], antheridia and archgonia were formed at about the same frequency in WT and Δ*SiR1* plants. Eight weeks after induction the first mature sporophytes were seen in WT plants, and after breaking the capsules the spores were set free (Fig. 6A). In the Δ*SiR1* lines, however, only one third of the number of sporophytes was formed (Table 2), and the spore capsules cracked open when the spores inside were still immature (Fig. 6B–D). These mutant spores did not germinate, revealing a strong effect of the disruption of *PpSiR1* on the reproductive cycle of *P. patens* and an unexpected link between sulfate assimilation and moss development.

3.5. Chloroplast structure and localization of sulfate assimilation enzymes

Since the disruption of *PpSiR1* did not greatly affect sulfate assimilation, we looked for alternative explanations of the developmental phenotypes. In higher plants SiR was shown to be involved in DNA binding in chloroplast nucleoids [33–35]. However, after DAPI staining no differences were observed between the nucleoid organisation in WT moss and the Δ*SiR1* plants under a confocal microscope (data not shown). Similarly, no significant alterations in chloroplast ultrastructure between WT moss and Δ*SiR1* 4–5 line were observed using transmission electron microscopy (Fig. 7a and

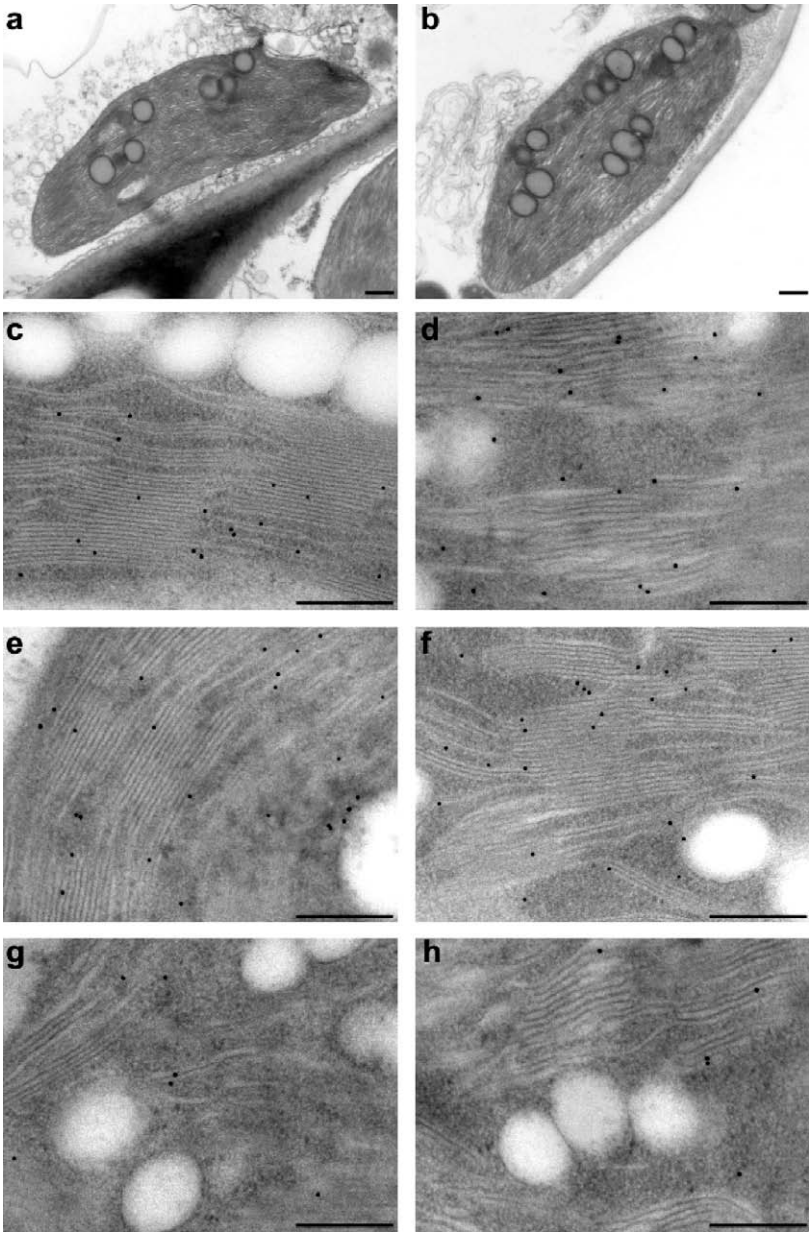

Fig. 7. Transmission electron microscopy and immunolocalization of enzymes of sulfate assimilation. Chloroplast ultrastructure of gametophores of wild type (a) and Δ*SiR1* 4–5 line (b). Immuno labeling with 10 nm protein A-gold of ATPS (c and d), APR (e and f) and SiR (g and h) in WT (c, e and g) and Δ*SiR1*4–5 line (d, f and h). Bar = 250 nm.

b). Because of the "spotty" pattern of SiR::GFP fusions (Fig. 1) and the known interactions between enzymes of sulfate assimilation [26,30] we hypothesized that lack of SiR1 might affect sublocalization of these proteins in the plastids. However, immunogold labeling with antisera against ATP sulfurylase, APR, and SiR did not detect any differences in the labeling patterns between WT and Δ*SiR1* 4–5 line (Fig. 7c–h). Despite SiR being often implicated in binding of chloroplast DNA, the immunolocalization did not indicate any preferential localization of SiR in nucleoids of *P. patens*.

4. Discussion

The disruption of the *SiR1* gene did not substantially affect sulfate assimilation in the protonema or gametophores of *P. patens*. Although expression of several genes was reduced in the Δ*SiR1* plants, the levels of thiols, sulfate uptake rates, and enzyme activities of ATP sulfurylase and APS reductase were not affected. Thiol levels often respond to manipulations of sulfate assimilation [36]. In *P. patens*, however, the pathway seems to be more robust, as disruption of neither of the two APS reductase isoforms, which possess the highest control over the pathway in *A. thaliana* [37], affected glutathione accumulation [11,22]. In addition, the Δ*SiR1* mutants were not sensitive to cadmium. Cadmium sensitivity is a typical consequence of unbalance in sulfate assimilation [11,22]. Rother et al. [38] showed a nearly 10-fold elevation of the *PpSiR2* transcript after treatment with 10 μM $CdCl_2$, however the two other isoforms were not analysed. Our results indicate a differential regulation of *PpSiR1* and *PpSiR2* upon cadmium exposure. Indeed, the level of SiR protein was not lower in the mutants than in wild type moss. As the transcripts levels of *SiR2* and *SiR3* were not elevated in the Δ*SiR1* mutants this compensation was most probably due to regulation at the translational level. It appears, therefore, that SiR is regulated on multiple levels, similar to other components of sulfate assimilation [25].

In contrast to Δ*APR* and Δ*APR-B* moss mutants [11,22] the Δ*SiR1* mutants displayed a remarkable developmental phenotype. The protoplast regeneration as well as the development of gametophores was retarded. The effect of *SiR1* disruption was strongest in the initial phase of development. Once a protonema or gametophore culture was established no significant differences between Δ*SiR1* and WT were observed in growth, content of low molecular weight thiols, redox state and cadmium tolerance. This phenotype of Δ*SiR1*, however, is different from described mutants in actin polymerization or cryptochrome signalling [39,40].

In further stages of the life cycle, Δ*SiR1* plants showed another developmental phenotype as they formed less sporophytes than wild type and their spore capsules opened before spore maturity. The maturity of spores is connected with colouring of the capsule and spores, changing during development from transparent to yellow-brownish and to brown when mature [12,41]. However, once the spore capsules of Δ*SiR1* were open, the spores inside did not change their colour. Consequently, the spores from these open but immature capsules are not able to germinate. Until now, disturbed sporophyte induction in *Physcomitrella* was described only for moss mutants constructed by deletion of genes essential for the formation of embryos or sporophytes in vascular plants-like *FLO/LFY*, *MIKC*-like *MADS-box* or *KNOX* [41–43] as well as *RAD51*, an important player in DNA repair [44]. In contrast to these genes, a connection between disruption of *SiR1* and control of sporophyte formation is difficult to explain. Possible explanations include a limitation in sulfur-containing metabolites, an alternative function of SiR in chloroplast DNA packaging, or a disruption of chloroplast ultrastructure. None of these hypotheses were, however, supported by the analyses of the Δ*SiR1* mutants. Neither metabolite contents nor cadmium sensitivity revealed any indication that sulfate assimilation is disrupted in the mutants. Similarly, DAPI staining and SiR immunolocalization did not provide any support for its function in DNA packaging in the moss. Thus, the mechanism by which disruption of *SiR1* causes the developmental phenotype remains to be elucidated. Although expression analysis provided no indication for specific function of SiR1 in sporophytes, tissue specific effects of the gene disruption cannot be excluded, because sporophyte metabolism is at least partially independent from that of the gametophyte [45]. Whether the developmental phenotype is specific for loss of function of *SiR1* or a generally for any SiR isoform will have to be elucidated by future analysis of plants lacking *SiR2* and *SiR3*.

The localization of SiR::GFP fusions revealed that the signal was not evenly distributed within the plastids but showed a spotty pattern as found earlier for APR, but not for APR-B [20]. This observation suggests an association of APR and SiR in a plastid subcompartment, similar to the specific localization of APR and SiR around the pyrenoid in *Chlamydomonas* plastids [26]. Other enzymes of sulfate assimilation may also be part of this complex, as protein–protein interactions between APR and ATP sulfurylase from onion were clearly established [30]. However, immunogold localization did not support this hypothesis because the labeling patterns for all three antisera, i.e. ATP sulfurylase, APR, and SiR, were uniformly distributed within the moss plastids. The immunolocalization of SiR, however, helped to address another intriguing question. In higher plants, SiR has been assigned an additional function in binding of chloroplast DNA in nucleoids [33–35]. The spotty pattern of localization of the GFP fusion constructs may reflect this chloroplast DNA compacting activity, as shown in pea chloroplasts with indirect immunofluorescence microscopy [46]. These two functions of SiR seem not to be exclusive, because the enzymatic activity of SiR was not affected by the binding to DNA [46]. However, we found no indication for a specific association of SiR with plastid DNA in *P. patens*. Apparently, this alternative function of SiR is a relatively new development in flowering plants or it is not a general but rather a species-specific feature [46,47].

In conclusion, the analysis of Δ*SiR1* mutants indicates a new function of SiR in moss development, independent from its enzymatic role in sulfate assimilation. In contrast to flowering plants, where SiR is also a multi-functional protein, apparently this function is not the packaging of plastidic DNA but an alternative function in process(es) essential for developmental control of regeneration and reproduction.

Acknowledgements

This work was supported by the German Research Foundation (DFG) grant KO2065/3 within the research group FOR 383 "Sulfur metabolism in plants: junction of basic metabolic pathways and molecular mechanisms of stress resistance". We thank Ursula Scheerer for performing the HPLC analysis and Anne Katrin Prowse for proofreading the manuscript. The research in SK's laboratory is supported by the UK Biotechnology and Biological Sciences Research Council.

Appendix A. Supplementary data

Supplementary data associated with this article can be found, in the online version, at doi:10.1016/j.febslet.2010.03.034.

References

[1] Cove, D., Bezanilla, M., Harries, P. and Quatrano, R. (2006) Mosses as model systems for the study of metabolism and development. Annu. Rev. Plant Biol. 57, 497–520.

[2] Lang, D., Zimmer, A.D., Rensing, S.A. and Reski, R. (2008) Exploring plant biodiversity: the *Physcomitrella* genome and beyond. Trends Plant Sci. 13, 542–549.
[3] Schäfer, D.G. and Zrÿd, J.-P. (1997) Efficient gene targeting in the moss *Physcomitrella patens*. Plant J. 11, 1195–1206.
[4] Hohe, A., Egener, T., Lucht, J., Holtorf, H., Reinhard, C., Schween, G. and Reski, R. (2004) An improved and highly standardised transformation procedure allows efficient production of single and multiple targeted gene knockouts in a moss, *Physcomitrella patens*. Curr. Genet. 44, 339–347.
[5] Kamisugi, Y., Schlink, K., Rensing, S.A., Schween, G., von Stackelberg, M., Cuming, A.C., Reski, R. and Cove, D.J. (2006) The mechanism of gene targeting in *Physcomitrella patens*: homologous recombination, concatenation and multiple integration. Nucleic Acids Res. 34, 6205–6214.
[6] Rensing, S.A., Fritzowsky, D., Lang, D. and Reski, R. (2005) Protein encoding genes in an ancient plant: analysis of codon usage, retained genes and splice sites in a moss, *Physcomitrella patens*. BMC Genomics 6, 43.
[7] Quatrano, R.S., Mc Daniel, S.F., Khandelwal, A., Perroud, P.F. and Cove, D.J. (2007) *Physcomitrella patens*: mosses enter the genomic age. Curr. Opin. Plant Biol. 10, 182–189.
[8] Kamisugi, Y., von Stackelberg, M., Lang, D., Care, M., Reski, R., Rensing, S.A. and Cuming, A.C. (2008) A sequence-anchored genetic linkage map for the moss *Physcomitrella patens*. Plant J. 56, 855–866.
[9] Rensing, S.A., Lang, D., Zimmer, A.D., et al. (2008) The *Physcomitrella* genome reveals insights into the conquest of land by plants. Science 319, 64–69.
[10] Girke, T., Schmidt, H., Zähringer, U., Reski, R. and Heinz, E. (1998) Identification of a novel Delta 6 acyl-group desaturase by targeted gene disruption in *Physcomitrella patens*. Plant J. 15, 39–48.
[11] Koprivova, A., Meyer, A.J., Schween, G., Herschbach, C., Reski, R. and Kopriva, S. (2002) Functional knockout of the 5′-phosphosulfate reductase gene in *Physcomitrella patens* revives an old route of sulfate assimilation. J. Biol. Chem. 227, 32195–32201.
[12] Hohe, A., Rensing, S.A., Mildner, M., Lang, D. and Reski, R. (2002) Day length and temperature strongly influence sexual reproduction and expression of a novel MADS-box gene in the moss *Physcomitrella patens*. Plant Biol. 4, 595–602.
[13] Reski, R. (1998) Development, genetics, and molecular biology of mosses. Bot. Acta 111, 1–15.
[14] Schween, G., Gorr, G., Hohe, A. and Reski, R. (2003) Unique tissue-specific cell cycle in *Physcomitrella*. Plant Biol. 5, 50–58.
[15] Thelander, M., Olsson, T. and Ronne, H. (2005) Effect of energy supply on filamentous growth and development in *Physcomitrella patens*. J. Exp. Bot. 56, 653–662.
[16] Decker, E.L., Frank, W., Sarnighausen, E. and Reski, R. (2006) Moss systems biology en route: phytohormones in *Physcomitrella* development. Plant Biol. 8, 397–406.
[17] Koprivova, A., Stemmer, C., Altmann, F., Hoffmann, A., Kopriva, S., Gorr, G., Reski, R. and Decker, E.L. (2004) Targeted knockouts of *Physcomitrella* lacking plant-specific immunogenic N-glycans. Plant Biotechnol. J. 2, 517–523.
[18] Stumpe, M., Bode, J., Göbel, C., Wichard, T., Schaaf, A., Frank, W., Frank, M., Reski, R., Pohnert, G. and Feussner, I. (2006) Biosynthesis of C9-aldehydes in the moss *Physcomitrella patens*. Biochim. Biophys. Acta 1761, 301–312.
[19] Kopriva, S., Wiedemann, G. and Reski, R. (2007) Sulfate assimilation in basal land plants-what does genomic sequencing tell us? Plant Biol. 9, 556–564.
[20] Kopriva, S., Fritzenmeier, K., Wiedemann, G. and Reski, R. (2007) The putative moss 3′-phosphoadenosine-5′-phosphosulfate reductase is a novel form of adenosine-5′-phosphosulfate reductase without an iron-sulfur cluster. J. Biol. Chem. 282, 22930–22938.
[21] Lang, D., Eisinger, J., Reski, R. and Rensing, S.A. (2005) Representation and high-quality annotation of the *Physcomitrella patens* transcriptome demonstrates a high proportion of proteins involved in metabolism in mosses. Plant Biol. 7, 238–250.
[22] Wiedemann, G., Koprivova, A., Schneider, M., Herschbach, C., Reski, R. and Kopriva, S. (2007) The role of the novel adenosine 5′-phosphosulfate reductase in regulation of sulfate assimilation of *Physcomitrella patens*. Plant Mol. Biol. 65, 667–676.
[23] Reski, R. and Abel, W.O. (1985) Induction of budding on chloronemata and caulonemata of the moss, *Physcomitrella patens*, using isopentenyladenine. Planta 165, 354–358.
[24] Strepp, R., Scholz, S., Kruse, S., Speth, V. and Reski, R. (1998) Plant nuclear gene knockout reveals a role in plastid division for the homolog of the bacterial cell division protein FtsZ, an ancestral tubulin. Proc. Natl. Acad. Sci. USA 95, 4368–4373.
[25] Koprivova, A., North, K.A. and Kopriva, S. (2008) Complex signaling network in regulation of adenosine 5′-phosphosulfate reductase by salt stress in *Arabidopsis* roots. Plant Physiol. 146, 1408–1420.
[26] Patron, N.J., Durnford, D.G. and Kopriva, S. (2008) Sulfate assimilation in eukaryotes: fusions, relocations and lateral transfers. BMC Evol. Biol. 8, 39.
[27] Kircher, S., Kozmar-Bognar, L., Kim, L., Adam, E., Harter, K., Schäfer, E. and Nagy, F. (1999) Light quality-dependent nuclear import of the plant photoreceptors phytochrome A and B. Plant Cell 11, 1445–1456.
[28] Kiessling, J., Kruse, S., Rensing, S.A., Harter, K., Decker, E.L. and Reski, R. (2000) Visualization of a cytoskeleton-like FtsZ network in chloroplasts. J. Cell Biol. 151, 945–950.
[29] Ye, F., Gierlich, J., Reski, R., Marienfeld, J. and Abel, W.O. (1989) Isoenzyme analysis of cytokinin sensitive mutants of the moss *Physcomitrella patens*. Plant Sci. 64, 203–212.
[30] Cumming, M., Leung, S., McCallum, J. and McManus, M.T. (2007) Complex formation between recombinant ATP sulfurylase and APS reductase of *Allium cepa* (L.). FEBS Lett. 581, 4139–4147.
[31] Tognetti, V.B., Palatnik, J.F., Fillat, M.F., Melzer, M., Hajirezaei, M., Valle, E.M. and Carrillo, N. (2006) Functional replacement of ferredoxin by a cyanobacterial flavodoxin in tobacco confers broad-range stress tolerance. Plant Cell 18, 2035–2050.
[32] Koprivova, A., Melzer, M., von Ballmoos, P., Mandel, T., Brunold, C. and Kopriva, S. (2001) Assimilatory sulfate reduction in C3, C3–C4, and C4 species of *Flaveria*. Plant Physiol. 127, 543–550.
[33] Sato, N., Nakayama, M. and Hase, T. (2001) The 70-kDa major DNA-compacting protein of the chloroplast nucleoid is sulfite reductase. FEBS Lett. 487, 347–350.
[34] Sekine, K., Hase, T. and Sato, N. (2002) Reversible DNA compaction by sulfite reductase regulates transcriptional activity of chloroplast nucleoids. J. Biol. Chem. 277, 24399–24404.
[35] Phinney, B.S. and Thelen, J.J. (2004) Proteomic characterization of a triton-insoluble fraction from chloroplasts defines a novel group of proteins associated with macromolecular structures. J. Proteome Res. 4, 497–506.
[36] Rennenberg, H., Herschbach, C., Haberer, K. and Kopriva, S. (2007) Sulfur metabolism in plants: are trees different? Plant Biol. 9, 620–637.
[37] Vauclare, P., Kopriva, S., Fell, D., Suter, M., Sticher, L., von Ballmoos, P., Krähenbühl, U., Op den Camp, R. and Brunold, C. (2002) Flux control of sulphate assimilation in *Arabidopsis thaliana*: adenosine 5′-phosphosulphate reductase is more susceptible to negative control by thiols than ATP sulphurylase. Plant J. 31, 729–740.
[38] Rother, M., Krauss, G.-J. and Wesenberg, D. (2006) Sulphate assimilation under Cd^{2+} stress in *Physcomitrella patens* – combined transcript, enzyme and metabolite profiling. Plant Cell Environ. 29, 1801–1811.
[39] Harries, P.A., Pan, A. and Quatrano, R.S. (2005) Actin-related protein2/3 complex component ARPC1 is required for proper cell morphogenesis and polarized cell growth in *Physcomitrella patens*. Plant Cell 17, 2327–2339.
[40] Perroud, P.F. and Quatrano, R.S. (2008) BRICK1 is required for apical cell growth in filaments of the moss *Physcomitrella patens* but not for gametophore morphology. Plant Cell 20, 411–422.
[41] Singer, S.D. and Ashton, N.W. (2007) Revelation of ancestral roles of KNOX genes by functional analysis of *Physcomitrella* homologues. Plant Cell Rep. 26, 2039–2054.
[42] Tanahashi, T., Sumikawa, N., Kato, M. and Hasebe, M. (2005) Diversification of gene function: homologs of the floral regulator FLO/LFY control the first zygotic cell division in the moss *Physcomitrella patens*. Development 132, 1727–1736.
[43] Singer, S.D., Krogan, N.T. and Ashton, N.W. (2007) Clues about the ancestral roles of plant MADS-box genes from a functional analysis of moss homologues. Plant Cell Rep. 26, 1155–1169.
[44] Markmann-Mulisch, U., Wendeler, E., Zobell, O., Schween, G., Steinbeiss, H.-H. and Reiss, B. (2007) Differential requirements for RAD51 in *Physcomitrella patens* and *Arabidopsis thaliana* development and DNA damage repair. Plant Cell 19, 3080–3089.
[45] Courtice, G.R.M., Ashton, N.W. and Cove, D.J. (1978) Evidence for the restricted passage of metabolites into the sporophyte of the moss *Physcomitrella patens* (Hedw.). Br. Eur. J. Bryol. 10, 191–198.
[46] Sekine, K., Fujiwara, M., Nakayama, M., Takao, T., Hase, T. and Sato, N. (2007) DNA binding and partial nucleoid localization of the chloroplast stromal enzyme ferredoxin:sulfite reductase. FEBS J. 274, 2054–2069.
[47] Lewandowska, M. and Sirko, A. (2008) Recent advances in understanding plant response to sulfur-deficiency stress. Acta Biochim. Polon. 55, 457–471.